Geologie en Mijnbouw **73:** 315–321, 1994.

Strong ground motion computation of the 1992 Roermond earthquake, the Netherlands, from linear methods using locally recorded aftershocks

J.C. Gariel[1], C. Horrent[2], D. Jongmans[2] & T. Camelbeeck[3]

[1] *Institut de Protection et de Sûreté Nucléaire, Département de Protection de l'Environnement et des Installations, Bureau d'Evaluation des Risques Sismiques pour la Sûreté des Installations Nucléaires, IPSN/CEA, BP 6, 92265 Fontenay-aux-Roses Cedex, France;* [2] *Laboratoire de Géologie de l'Ingénieur, Liège University, Bat B 19, 4000 Liège, Belgium;* [3] *Observatoire Royal de Belgique, Avenue Circulaire 3, 1180 Bruxelles, Belgium*

Received 16 June 1993; accepted in revised form 6 January 1994

Key words: empirical Green's function, convolution method, strong motion, peak ground acceleration

Abstract

The strong earthquake (M_L = 5.8) on April 13, 1992 near Roermond (the Netherlands) is the largest for the area in the last 50 years and has affected a highly urbanized and industrialized region. Unfortunately, no strong motion records were retrieved in the epicentral area. However, a temporary network was installed by the Belgium Royal Observatory a few hours after the mainshock and more than 100 aftershocks were recorded by digital stations. These aftershock records are used to reconstruct the ground motion in the epicentral area during the mainshock. Two different techniques have been considered, namely the empirical Green's function method and the convolution technique. Using the former one, it is shown that, in the epicentral area, peak acceleration reached values between 0.57 and 1.75 m/s^2. Acceleration values two times larger are obtained using the deconvolution technique.

Introduction

On April 13, 1992, a strong earthquake (M_L = 5.8) occurred a few kilometers south-west of the city of Roermond (the Netherlands). This earthquake is the largest in this region in the last 50 years and it has affected a highly urbanized and industrialized region of northwest Europe. Unfortunately, no strong motion records were retrieved in the epicentral area and only macroseismic intensities (VII in the epicentral region, Ahorner 1992) were available to quantify strong ground motion. However, a temporary network was deployed by the Belgium Royal Observatory a few hours after the mainshock. More than 100 aftershocks were then recorded by seven digital stations located between 5 and 15 km from the epicenter (Camelbeeck et al. 1994). In this study, we take advantage of this near-field dataset to reconstruct strong ground motion in the epicentral area during the mainshock. We use two different techniques: the empirical Green's function method and the convolution method.

Data

Roermond is located in the Lower Rhine Graben, an active NW–SE oriented rift zone. In this area important variations in the sedimentary cover (Mesozoic, Cenozoic and Quaternary) are observed. The thickness of this cover varies from 1500 m under Roermond city to less than 500 m a few kilometers north-east of the city. In the past, several large earthquakes have been observed in this region. The focal mechanism of the Roermond earthquake agrees with the normal faulting observed in this area (Ahorner 1992).

The permanent Belgian seismic network comprises 21 digital stations. Among them, about one half are equipped with three-component seismometers (Fig. 1). Due to the limited dynamic range of the instruments, all records from stations located at less than 100 km were saturated. That located at Vianden (VIA, Luxembourg) is the Belgian station closest to the epicenter (138 km) which did not saturate. As most of the aftershocks were also recorded at this particular station, these data

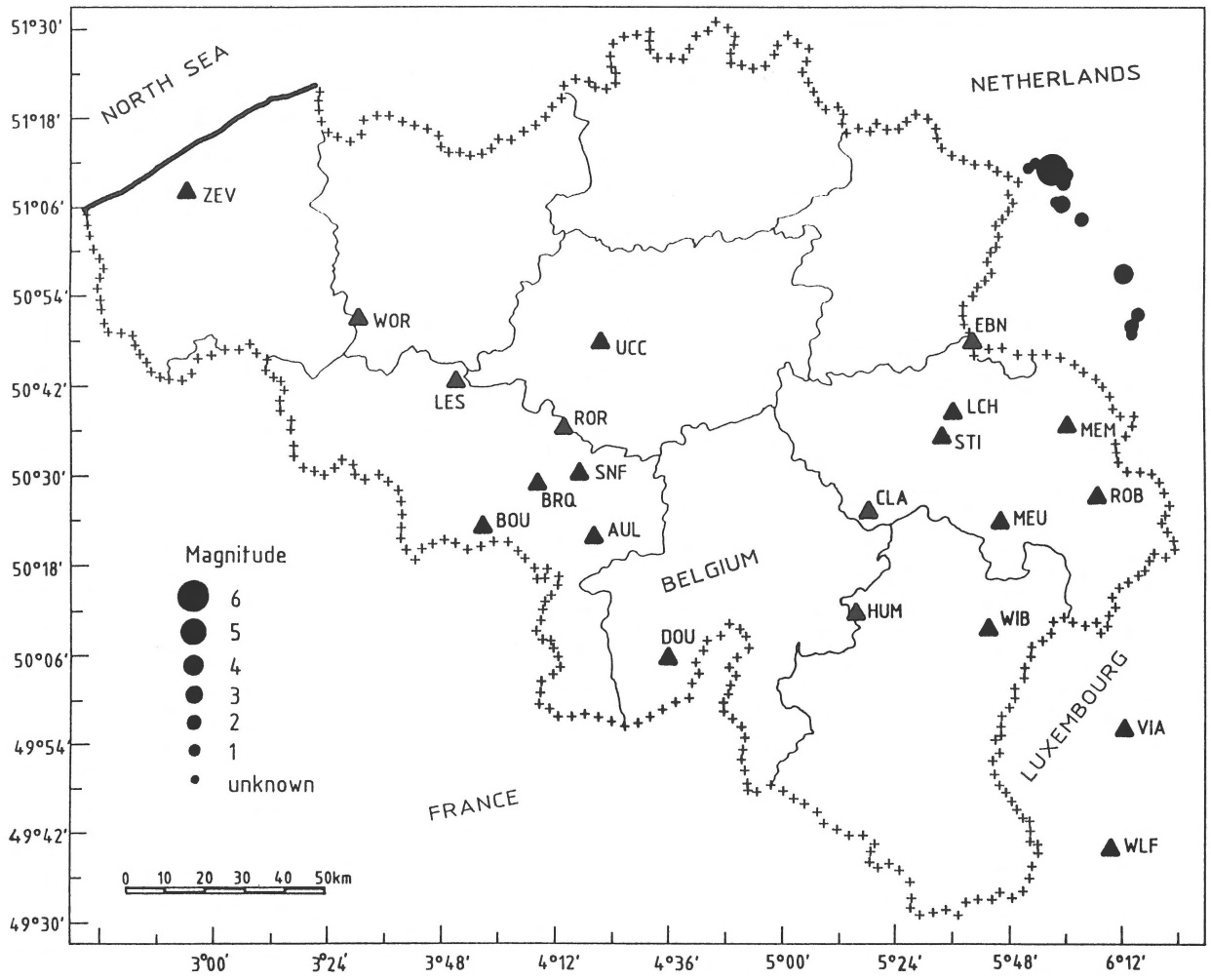

Fig. 1. Location of the stations of the Belgian permanent network (▲). The epicenter of the 1992 Roermond mainshock and several aftershocks are indicated by black dots, scaled according to magnitude (M_L).

have been selected to calibrate the empirical Green's function technique.

Approximatively five hours after the mainshock, the Belgium Royal Observatory team installed seven digital stations equipped with 3-component seismometers at epicentral distances ranging from 5 to 15 km (Fig. 2). More than 100 aftershocks were recorded by this temporary network and 55 were located with an epicentral accuracy better than one km (Camelbeeck et al. 1994). The largest aftershock (M_L = 4.0) occurred about 20 km south-east of the mainshock epicenter. The distribution of the hypocenter defines a plane striking N120° and dipping 70°. This is in good agreement with one of the nodal planes of the fault plane solution for the mainshock (Camelbeeck et al. 1994). It is also worth noticing that some aftershocks define a plane parallel to that of the mainshock, but shifted to the west. The mainshock epicenter is located at the north end of the plane defined by the aftershock distribution, suggesting an unilateral propagation of the rupture from the north-west to the south-east.

Methods

Empirical Green's function method

This technique, initially introduced by Hartzell (1978), has been modified and improved by several authors (Irikura 1983, 1986, Joyner & Boore 1986, Boatwright

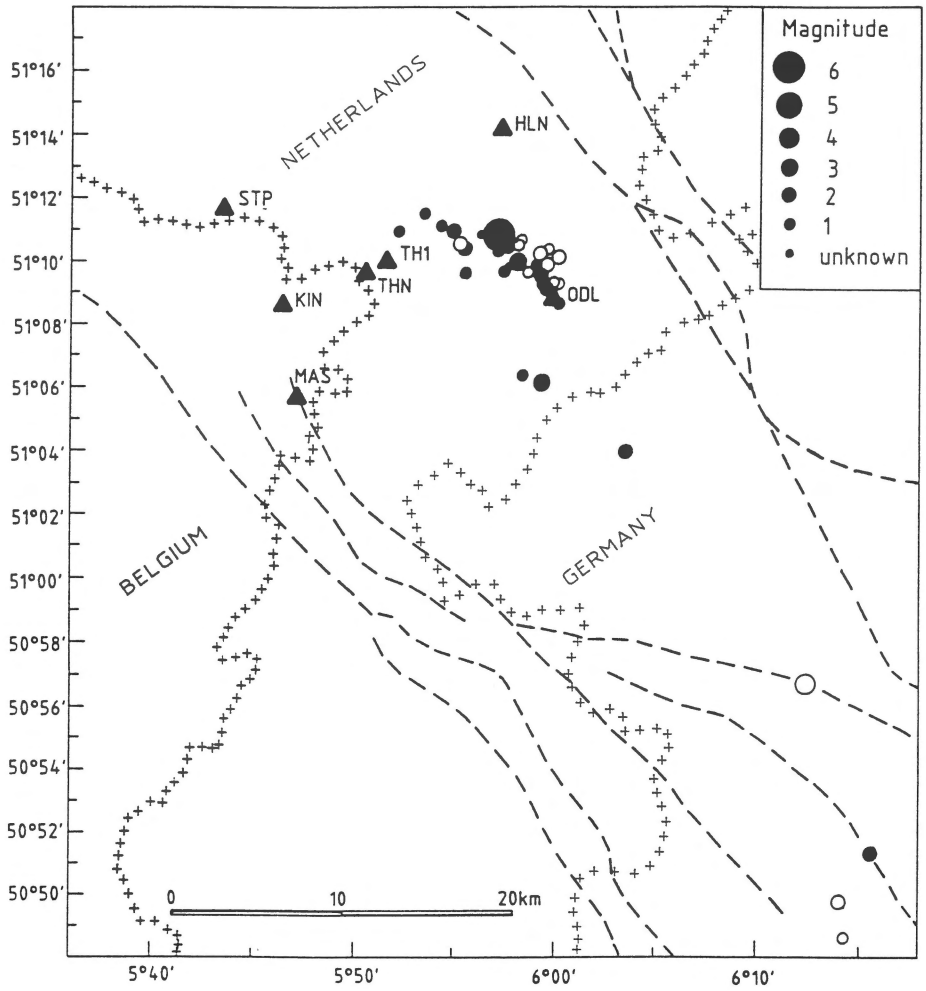

Fig. 2. Location of the stations of the temporary Belgian network (▲). The epicenters of the mainshock and several aftershocks are indicated by black dots and open circles. Dashed lines indicate faults, crosses indicate national borders.

1988, Wennerberg 1990, and others). Basically, the empirical Green's function technique uses small seismic event records as Green's function. One of the major advantages of this method is that both propagation and site effects are explicitly included in the small event recording.

Let us assume that the seismic moment of the event to be simulated (target event) is N^3 larger than that of the small event. The fault plane of the target event can be divided into N by N elements, each of them representing the small event. If we assume that the stress-drop is similar for both the small and the target event, the ground motion $A(t)$ associated with the target event can be expressed as a function of the ground motion associated with the small event $a(t)$ by the following expression:

$$A(t) = \sum_{i=1}^{N^2} \left[\frac{r}{r_i}\right] F_i(t) * a(t) \qquad (1)$$

where r is the hypocentral distance of the small event, r_i is the distance between the observation point and the ith fault element and * the convolution operator. $F_i(t)$ is a filter which allows to adjust the difference between the source time functions associated with the target and the small event. It is dependent on the distance between the initiation point of the rupture and the ith fault element, the rupture velocity, the seismic wave velocity in the crust and the rise-time of the small event. In this formulation, the low-frequency part of the small event spectrum is summed N^3 times (coherent summation), allowing to retrieve the correct

moment for the target event. At high frequency, the spectral level is proportional to the square root of the N^2 summations (non-constructive summation). As a consequence, the spectral amplitude at high frequency will be proportional to the cubic root of the amplitude at low frequency, which is in agreement with the similarity law imposed by the 'omega-square' model (Irikura 1986). More details about this method can be found in Gariel et al. (1993).

Convolution method

The convolution technique is based on the following linear equation:

$$V_{M,1}(f) = \frac{V_{M,2}(f)}{V_{A,2}(f)} V_{A,1}(f) \qquad (2)$$

where $V_{M,1}$ and $V_{M,2}$ are the velocity spectra at stations 1 and 2 for the mainshock and $V_{A,1}$ and $V_{A,2}$ are the corresponding ones for the aftershock. Both earthquakes are supposed to be located at the same place and to have the same focal mechanism. Ideally, the ratio $V_{M,2}/V_{A,2}$ should correspond to a filter taking into account the differences between the source time functions of the mainshock and the aftershock.

Results

Empirical Green's function method

In a first step, we used records from a single station of the permanent Belgian network in order to check the validity of the technique. As mentioned above, station VIA was the closest station of the permanent network with unclipped records of the mainshock, and recorded most of the aftershocks. We used two of the aftershocks (with magnitude $M_L = 2.5$ and $M_L = 2.9$) as empirical Green's function to simulate the mainshock record. The two events were selected on the basis of their good signal to noise ratio, and also because they have a mechanism almost similar to that of the mainshock. Source sizes of the two aftershocks were deduced from Fourier spectra examination and corner frequency determination. Deduced source radii were respectively 0.16 and 0.2 km for the $M_L = 2.5$ and $M_L = 2.9$ events. In a second step, the total number of elementary faults constituting the fault plane of the target event has to be determined. This number N can be obtained through the computation of the ratio M_0/M_{0A}, where M_0 is the seismic moment of the mainshock ($M_0 = 8.10^{16}$ Nm in the case of the Roermond earthquake) and M_{0A} is the seismic moment of the aftershock under consideration. Practically, the evaluation of the ratio M_0/M_{0A} is difficult, because, first, it supposes that the target and the small events have a similar stress-drop (which is rarely the case), and second, the determination of the seismic moment of the small event is difficult. As both the target event and the small event records were available at station VIA, N has been obtained through a trial and error process. Several other calculations have been performed in order to evaluate the influence of the rupture velocity. In all these computations, it was assumed that the rupture initiated at the lower north-western corner of the fault plane as was suggested by the aftershock distribution. The main parameters of the computation are summarized in Table 1. The deduced parameters of the Roermond earthquake are:

- Length: 2 km,
- Width: 2.2 km,
- Rise-time: 0.1 s,
- Rupture velocity = 2000 m/s.

Using the summation parameters obtained at station VIA, we computed ground motions at most of the stations of the temporary network in the epicentral area. Due to the sensor response (natural frequency around 1 Hz), resulting time series were bandpass filtered between 0.5 and 10 Hz. Because of the small distance between the fault and the recording sites, station azimuth relative to the rupture front varies rapidly inducing a possible influence of the radiation pattern on the summation process. In order to minimize this effect, the radiation factor of each elementary fault has been corrected according to its position relative to the station. Figure 3 shows an example of the resulting time series at two stations: ODL which is located just above the fault plane and KIN located about 12 km west of the epicenter. One can notice the short duration of strong acceleration (a few seconds) which has

Table 1. Parameters used in the empirical Green's function simulation of the Roermond earthquake.

Aftershock date	M_L	Radius (km)	Rise time (s)	N^3	Mechanism ϕ, θ, λ
92 0414 1241	2.5	0.16	0.008	1100	124 46 – 118
92 0502 0850	2.9	0.20	0.01	1872	139 75 – 96

ϕ – azimuth, θ – dip and λ – rake; N – number of elementary sources; M_L – local Richter magnitude.

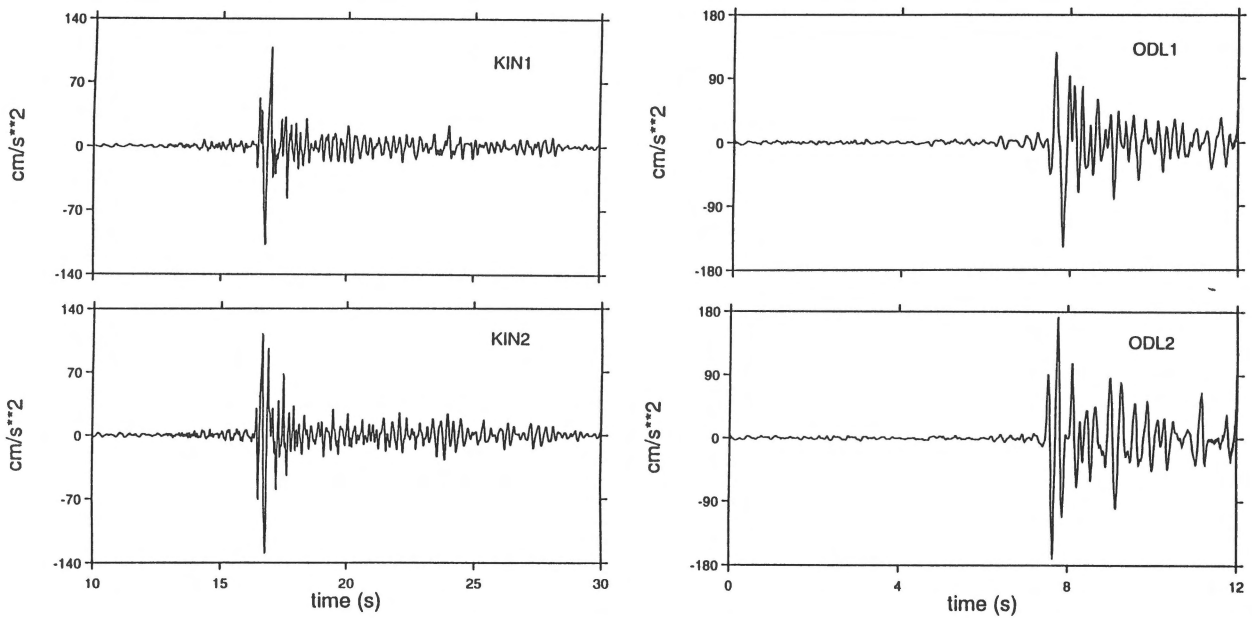

Fig. 3. Synthetic horizontal accelerograms for the Roermond mainshock obtained by the empirical Green's functions technique at stations ODL and KIN (two components).

to be related to the relatively small size of the source and to the small hypocentral distances. Peak ground acceleration values obtained at six stations of the temporary network are summarized in Table 2. At station HLN, one may notice a very large peak acceleration (3.5 m/s^2). HLN is located in Haelen, where the most significant damage has been reported. In particular, one of the turbines of the local power plant moved during the mainshock. This is in agreement with the large peak acceleration obtained by the empirical Green's function technique. However, one should keep in mind that the fundamental assumption of this method is the linear behavior of the geological formations. In the case of Haelen, which is located in the alluvial Rhine graben embayment, possible non-linear effects could have reduced the actual acceleration level. This large value might also be explained by some peculiar radiation pattern effects. Peak ground accelerations obtained at the other stations range between 0.57 and 1.75 m/s^2, in agreement with what should be expected for a magnitude 5.8 event. Examples of response spectra associated with the obtained time series are shown in Fig. 4. Predominant frequencies of these spectra are in the range 2.0 to 5.0 Hz and are probably associated with local geological conditions.

Table 2. Calculated peak ground acceleration in m/s^2 for two horizontal components (comp. 1 and comp. 2). For station locations see Fig. 2.

Station	ODL	HLN	THN	KIN	STP	MAS
Epicentral distance (km)	5.0	6.2	8.6	13.4	14.8	15.1
Comp. 1	1.50	1.74	0.60	1.10	–	0.80
Comp. 2	1.75	3.50	0.72	1.30	1.20	0.57

Convolution method

As both the mainshock and most of the aftershocks were recorded at VIA, we used records from this station to compute the ratio function described in equation (2). Figure 5 shows the observed time series (horizontal transverse component) for both the mainshock and the selected aftershock, the result of their ratio and the associated Fourier spectra. Using the source function ratio and equation (2), the ground motions were computed in the frequency range 2.0–10.0 Hz at the different stations of the temporary network. The resulting seismogram and accelerogram at station KIN are shown on Fig. 5A. Peak acceleration reaches about

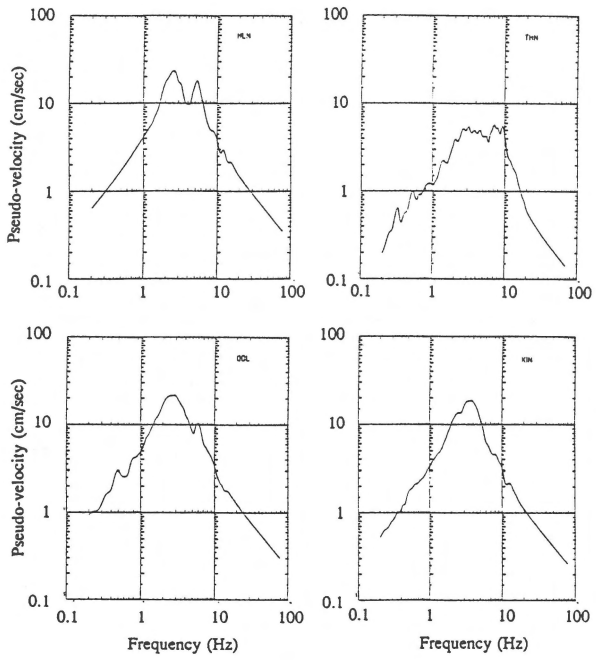

Fig. 4. Response spectra (5% damping) of horizontal accelerograms computed from recorded seismograms at stations HLN, THN, ODL and KIN.

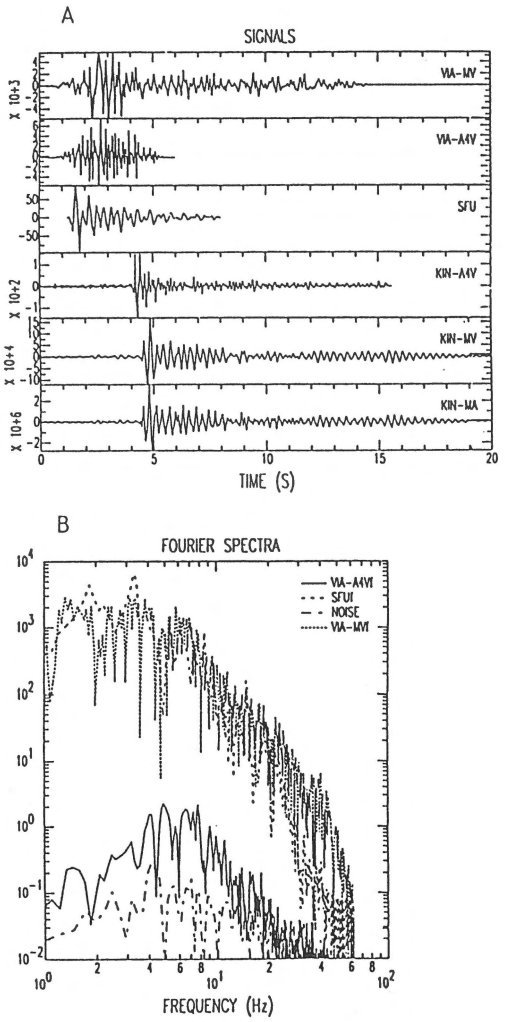

Fig. 5. (A) Recorded and computed seismograms/accelerograms at stations VIA and KIN. Amplitudes are in μm/s for seismograms and μm/s^2 for accelerograms. From top to bottom:– Recorded horizontal seismogram at VIA for the mainshock (VIA-MV),– Recorded horizontal seismogram at VIA for an aftershock (VIA-A4V),– Deconvolved source function (SFU) for the mainshock,– Recorded horizontal seismogram at KIN for an aftershock (KIN-A4V),– Computed horizontal seismogram at KIN for the mainshock (KIN-MV),– Computed horizontal accelerogram at KIN for the mainshock (KIN-MA), (B) Fourier spectra of:– Horizontal seismogram at VIA for the mainshock (VIA-MVf),– Horizontal seismogram at VIA for an aftershock (VIA-A4Vf),– Deconvolved source function (SFUf) for the mainshock,– Noise at VIA before the aftershock (NOISE).

2.5 m/s^2, which is about twice the value obtained from the empirical Green's function technique. Although the two methods are based on the same assumption (linearity), similar overestimations were observed at all the stations.

The critical point in equation (2) is the spectral ratio computation at the reference station. Fourier spectra of the mainshock and the aftershock exhibit very different shapes due to the different sizes of the events (Fig. 5B). For the mainshock, most of the energy is in the frequency range 1.0–4.0 Hz, whereas the aftershock spectrum contains most of its energy in the frequency band 4.0–8.0 Hz with minima at 1.9 and 3.4 Hz. This explains why the spectral ratio shows large maxima for these two specific frequencies. Filtering and/or smoothing of the spectra does not significantly decrease acceleration level as low-frequency energy is boosted when computing the spectral ratio. The poor signal to noise ratio which characterizes the aftershock signal (Fig. 5) might also explain part of the erroneous estimation obtained from the convolution method.

Attenuation of ground motion with distance

In order to study the attenuation of peak acceleration with distance, we applied the empirical Green's function technique for all the clipped stations of the permanent Belgian network. For stations with unclipped

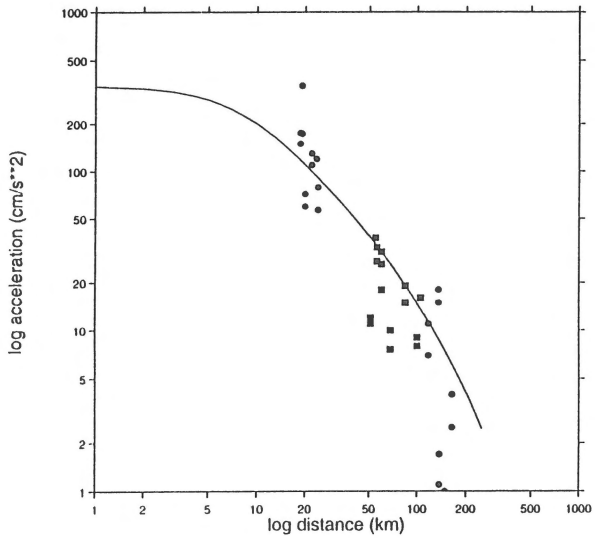

Fig. 6. Comparison between peak acceleration attenuation law proposed by Boore & Joyner (1982) for an $M_L = 5.8$ earthquake and the observed and computed peak acceleration values in Belgium (•) and Germany (■) (from Ahorner 1992).

seismograms, ground accelerations were obtained by removing the instrumental response and taking the derivative of the ground velocity. Figure 6 presents peak acceleration values at all Belgian stations as a function of distance. Peak accelerations from German stations (Ahorner 1992) were also added on the plot. These values are compared with the empirical attenuation relationship from Boore & Joyner (1982). Peak acceleration for the closest stations are scattered suggesting a probable influence of source or/and site effects. Peak acceleration for distances larger than 100 km are lower, suggesting a stronger attenuation.

Conclusion

Using the empirical Green's function method, acceleration levels in the epicentral region of the Roermond earthquake were estimated. Highest peak acceleration reaching 3.5 m/s^2 was found north-east of the epicenter at Haelen where intensity VII was observed. This estimate should be balanced because of the linearity assumption inherent to the method. For five other stations, we find estimated ground accelerations between 0.57 and 1.75 m/s^2 for epicentral distances ranging between 5 and 15 km. In spite of these acceleration levels, one may be surprised by the relatively small amount of damage reported. This could be explained first by the nature of the seismic motion, i.e. a relatively short duration of the strong motion, and second by the quality of the constructions which limited the damage significantly.

Peak accelerations obtained from the convolution method are about two times larger than those estimated by the empirical Green's function method. This is probably due to the difference in the predominant frequencies between the mainshock and the aftershocks which affects strongly the spectral ratio computation.

This study shows that the empirical Green's function technique is a convenient tool to retrieve strong motion records from small event recordings. It is particularly suited for a region such as northwestern Europe where no permanent strong motion network exists but where temporary networks can be rapidly installed after a large event allowing to record most of the aftershocks.

References

Ahorner, L. 1992 Das Erdbeben bei Roermond am 13. April 1992 und die daraus zu ziehenden Lehren für das Erdbebengefahrdungspotential in Rheinland – Mitt. Deutsch. Geoph. Ges. 1–2: 51–57

Boatwright, J. 1988 The seismic radiation from composite models of faulting – Bull. Seism. Soc. Am. 78: 489–508

Boore, D.M. & W.B. Joyner 1982 The empirical prediction of ground motion – Bull. Seism. Soc. Am. 72: S43–S60

Camelbeeck, T., T. van Eck, L. Ahorner, R. Pelzing, J. Loohuis, T. Hoang-Trong & D. Hollnack 1994 The 1992 Roermond earthquake, the Netherlands, and its aftershocks – Geol. Mijnbouw, this issue

Gariel, J.C., C. Horrent, D. Jongmans & Th. Camelbeeck 1993 Etude des mouvements forts lors du séisme de Roermond du 13 avril 1992. Actes 3eme Colloque National AFPS 'Génie parasismique et aspects vibratoires dans le génie civil' I: ES-87, Saint-Remy-les-Chevreuse (France), 24–26 mars 1993

Hartzell, S.N. 1978 Earthquake aftershocks as Green's functions – Geophys. Res. Letters 5: 1–4

Irikura, K. 1983 Semi-empirical estimation of strong ground motions during large earthquakes – Bull. Disas. Prev. Res. Institute, Kyoto University, 33, Part 2, 298: 63–124

Irikura, K. 1986 Prediction of strong acceleration motions using empirical Green's functions, Proceedings seventh Jap. Earth. Eng. Symp.: 151–156

Joyner, W.B. & D.M. Boore 1986 On simulating large earthquakes by Green's function addition of small earthquakes. In: S. Das, J. Boatwright & C.H. Scholz (eds) Earthquake Source Mechanics – Geophysical Monograph 37 (Maurice Ewing series 6), American Geophysical Union, Washington D.C.: 269–274

Wennerberg, L. 1990 Stochastic summation of empirical Green's functions – Bull. Seism. Soc. Am. 80: 1414–1432